

12

LEVEL III

AD-E000384

NRL Report 8377

ADA 082795

Double-Ended Backward-Wave Yagi Hybrid Antenna

WALTER K. KAHN

*Airborne Radar Branch
Radar Division*

February 15, 1980

DTIC
ELECTE
APR 8 1980
S D
B



NAVAL RESEARCH LABORATORY
Washington, D.C.

Approved for public release; distribution unlimited.

DTIC FILE COPY

80 2 22 01

SECURITY CLASSIFICATION OF THIS PAGE (When Data Entered)

REPORT DOCUMENTATION PAGE		READ INSTRUCTIONS BEFORE COMPLETING FORM
1. REPORT NUMBER NRL Report 8377	2. GOVT ACCESSION NO.	3. RECIPIENT'S CATALOG NUMBER
4. TITLE (and Subtitle) DOUBLE-ENDED BACKWARD-WAVE YAGI HYBRID ANTENNA		5. TYPE OF REPORT & PERIOD COVERED Report on one phase of a continuing NRL problem number
		6. PERFORMING ORG. REPORT NUMBER
7. AUTHOR(s) Walter K. Kahn		8. CONTRACT OR GRANT NUMBER(s)
9. PERFORMING ORGANIZATION NAME AND ADDRESS Naval Research Laboratory Washington, DC 20375		10. PROGRAM ELEMENT, PROJECT, TASK AREA & WORK UNIT NUMBERS NRL Problem 53-0663-0 Project NAVAIR WF12-141-605
11. CONTROLLING OFFICE NAME AND ADDRESS Naval Air Systems Command Washington, DC 20361		12. REPORT DATE February 15, 1980
		13. NUMBER OF PAGES 10
14. MONITORING AGENCY NAME & ADDRESS (if different from Controlling Office)		15. SECURITY CLASS. (of this report) UNCLASSIFIED
		15a. DECLASSIFICATION/DOWNGRADING SCHEDULE
16. DISTRIBUTION STATEMENT (of this Report) Approved for public release: distribution unlimited.		
17. DISTRIBUTION STATEMENT (of the abstract entered in Block 20, if different from Report)		
18. SUPPLEMENTARY NOTES		
19. KEY WORDS (Continue on reverse side if necessary and identify by block number) Antennas Yagi antennas Surface-wave antennas Dipole arrays		
20. ABSTRACT (Continue on reverse side if necessary and identify by block number) A structurally simple antenna configuration, which offers lower sidelobe levels than a conventional Yagi, is described. The antenna combines a backward-wave excited array with a Yagi parasitically excited array of dipoles.		

DTIC
ELECTE
S APR 8 1980 D
B

DD FORM 1473
1 JAN 73

EDITION OF 1 NOV 65 IS OBSOLETE
S/N 0102-014-6601

i
SECURITY CLASSIFICATION OF THIS PAGE (When Data Entered)

CONTENTS

INTRODUCTION 1

ANALYSIS 1

A 16-ELEMENT ARRAY 4

ACKNOWLEDGMENTS 6

REFERENCES 6

ACCESSION for	
NTIS	White Section <input checked="" type="checkbox"/>
DOC	Buff Section <input type="checkbox"/>
UNANNOUNCED	<input type="checkbox"/>
JUSTIFICATION _____	
BY _____	
DISTRIBUTION/AVAILABILITY CODES	
Dist. A/REL and/or SPECIAL	
A	

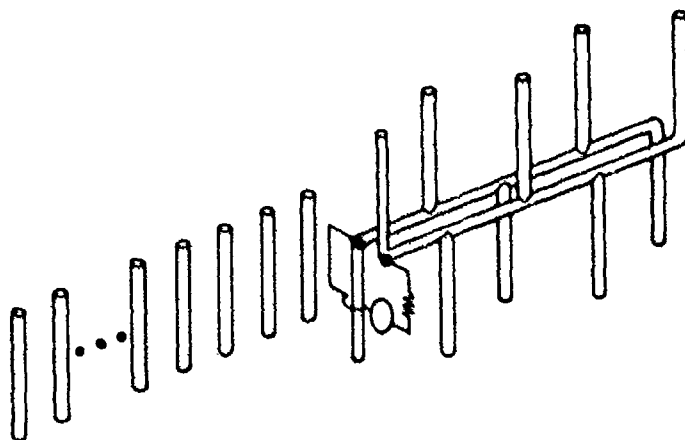


Fig. 1 -- Double-ended backward-wave Yagi hybrid antenna

DOUBLE-ENDED BACKWARD-WAVE YAGI HYBRID ANTENNA

INTRODUCTION

This report describes a novel dipole endfire array configuration on which the currents inherently tend to taper as required for low sidelobes [1]. In the conventional traveling-wave array designed for endfire, excitation is provided at one end of the array. The currents on a uniform array of elements tend to taper away from that end; other current distributions are obtained by changing the elements themselves or their coupling to the traveling-wave structure. In the proposed configuration (Fig. 1) excitation enters at a more medial point of the array, and conceptually the new antenna combines a backward-wave segment [2] with a forward-wave Yagi segment [3]. Currents on the medial element and elements adjoining this element (which is excited directly from the source) are enhanced by components usually lumped as (unavoidable) "feed radiation." An array of 16 dipoles chosen in accordance with this idea was computed to have a sidelobe level better than -20 dB at the design frequency and -16 dB over an 8% band. A conventional Yagi produces sidelobe levels of approximately -14 dB at the design frequency [4].

ANALYSIS

An equivalent circuit for the backward-wave Yagi hybrid antenna is shown in Fig. 2. The N -port feed network is shown at the left. Port 1 is the input. Ports 2 to $K + 1$ represent terminal pairs at which a backward-wave structure is connected to K dipole radiators. At ports $K + 2$ to $K + L + 1$, reactive terminations are connected to L Yagi director elements. The network at the right with $M = K + L$ ports represents radiation and mutual coupling of the array elements. Conditions at the n^{th} port will be described by a voltage V_n and a current I_n directed as shown on the diagram.

It will be convenient to group the currents I_n in two distinct ways, leading to two partitionings of the total currents matrix:

$$\underline{I} = \begin{bmatrix} I_1 \\ I_2 \\ \dots \\ I_N \end{bmatrix} = \begin{bmatrix} I_\alpha \\ I_\beta \end{bmatrix} = \begin{bmatrix} I_\nu \\ I_\mu \end{bmatrix} \quad (1)$$

where

$$\tilde{I}_\alpha = [I_1], \text{ dimension 1 by 1,}$$

KAHN

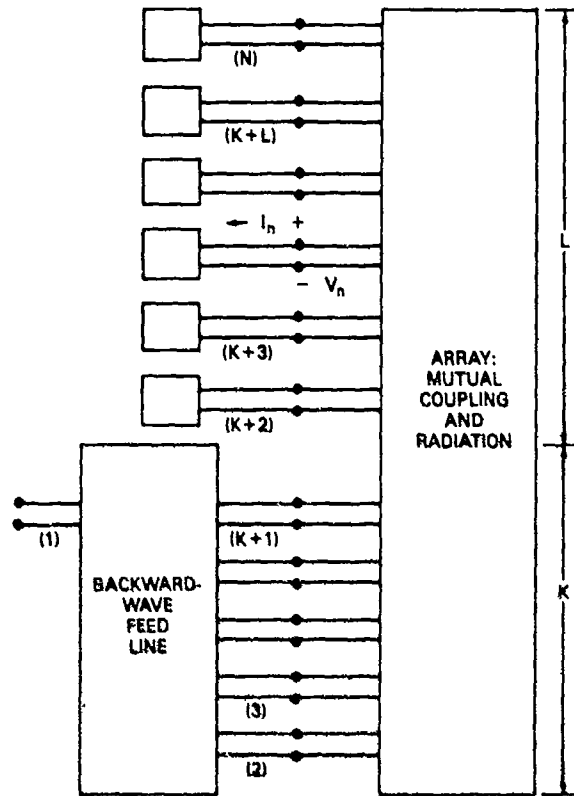


Fig. 2 -- Equivalent circuit for a backward-wave Yagi hybrid antenna

$$\tilde{I}_\theta = [I_2 \ I_3 \ \dots \ I_N], \text{ dimension } 1 \text{ by } M,$$

$$\tilde{I}_\nu = [I_1 \ I_2 \ \dots \ I_{K+1}], \text{ dimension } 1 \text{ by } K + 1,$$

$$\tilde{I}_\mu = [I_{K+2} \ I_{K+3} \ \dots \ I_N], \text{ dimension } 1 \text{ by } L,$$

with \sim denoting the transposed matrix. Voltage and impedance matrices are partitioned conformably.

The relation between voltages and currents of the feed network is governed by the impedance matrix Z :

$$\underline{V} = Z \underline{I} \quad (2a)$$

or

$$\begin{bmatrix} \underline{V}_\nu \\ \underline{V}_\mu \end{bmatrix} = \begin{bmatrix} Z_{\nu\nu} & Z_{\nu\mu} \\ Z_{\mu\nu} & Z_{\mu\mu} \end{bmatrix} \begin{bmatrix} \underline{I}_\nu \\ \underline{I}_\mu \end{bmatrix}, \quad (2b)$$

wherein the impedance matrix $Z_{\nu\nu}$ which characterizes the backward-wave circuit will be taken up in the next paragraph, $Z_{\nu\mu} = Z_{\mu\nu} = 0$, and $Z_{\mu\mu}$ is a diagonal matrix. The entries on the principal diagonal of $Z_{\mu\mu}$ are reactive terminations, $jX_{K+2}, \dots, jX_{K+L+1}$, at the ports of the Yagi directors. Equation (2a) may now be rewritten (using a different grouping of the elements) as

$$\begin{bmatrix} \underline{V}_\alpha \\ \underline{V}_\beta \end{bmatrix} = \begin{bmatrix} Z_{\alpha\alpha} & Z_{\alpha\beta} \\ Z_{\beta\alpha} & Z_{\beta\beta} \end{bmatrix} \begin{bmatrix} \underline{I}_\alpha \\ \underline{I}_\beta \end{bmatrix}. \quad (3)$$

Radiation and mutual coupling of the dipoles give the relation

$$\underline{V}_\beta = Z_A (-\underline{I}_\beta), \quad (4)$$

where the elements of Z_A are known [5,6]. Substituting in (3) yields

$$Z_A (-\underline{I}_\beta) = Z_{\beta\alpha} \underline{I}_\alpha + Z_{\beta\beta} \underline{I}_\beta \quad (5a)$$

or

$$-\underline{I}_\beta = (Z_{\beta\beta} + Z_A)^{-1} Z_{\beta\alpha} \underline{I}_\alpha. \quad (5b)$$

The (input) impedance of the array is obtained by eliminating \underline{I}_β from the first constituent of (3):

$$\underline{V}_\alpha = \left[Z_{\alpha\alpha} - Z_{\alpha\beta} (Z_{\beta\beta} + Z_A)^{-1} Z_{\beta\alpha} \right] \underline{I}_\alpha. \quad (6)$$

The radiation pattern is determined by the relative values of the antenna currents $-\underline{I}_\beta$, which can be found from (5b) by arbitrarily setting $\underline{I}_\alpha = 1$. It is obviously independent of any source impedance or precise value of input impedance.

We now return to the evaluation of $Z_{\nu\nu}$, the open-circuit impedance matrix of the backward-wave feed-line network. This network is shown in Fig. 3a, with Figs. 3b and 3c defining the circuit symbols used. The dipole elements are connected in shunt, forming a shunt three-port T junction at the terminal pairs marked 2, 3, ..., $K+1$. Figure 3b represents a lossless transmission line of length ℓ , characteristic resistance R_0 , and propagation

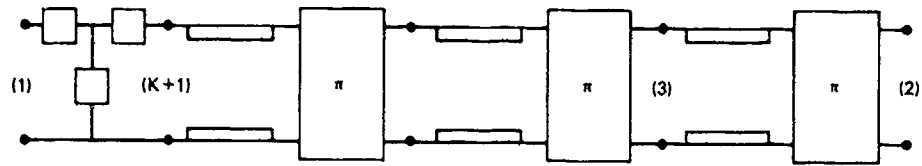


Fig. 3a — Backward-wave feed-line network

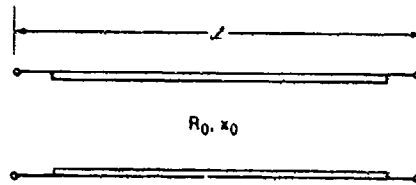
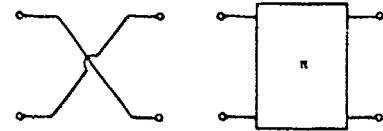


Fig. 3b — Transmission line

Fig. 3c — Phase-reversal network
schematized in two ways

constant κ_0 . For TEM lines, κ_0 would be proportional to frequency. In the antenna diagram (Fig. 1) the dipoles are shown attached to alternate conductors of the two-wire transmission line. This produces a reversal in excitation phase which can also be schematized in the two alternative ways shown in Fig. 3c: transposition of conductors and a length of transmission π electrical radians in length (independent of frequency) [7]. The two-port connecting the input (1) with the $(K + 1)$ th terminal pair merely alters the internal impedance of the source and does not alter the patterns. Although shown arbitrary, a (dummy) section of the backward-wave line was chosen for convenience. The open-circuit impedance matrix can now be calculated via a number of circuit techniques all leading to relative values of V_r and I_s : $Z_{rs} = V_r/I_s$, when $I_r = 0$ for all $r \neq s$.

A 16-ELEMENT ARRAY

As an illustration of these ideas the performance of a sixteen-element backward-wave Yagi array was computed. The array comprised a backward-wave structure of five dipoles spaced 0.260 m apart and eleven Yagi director dipoles spaced 0.4 m apart. The TEM two-wire transmission line of the backward-wave circuit had a characteristic resistance $R_0 = 300$. Each dipole rod had radius 0.024 m. The lengths of the dipoles are given in Table 1 (in order from the backward-wave end to the front of the Yagi).

The computations were carried out using the formulas for mutual coupling among canonical minimum-scattering (CMS) antennas supplemented by a (separately evaluated) antenna impedance [6,8]. The equivalent circuit for implementing this calculation is shown in Fig. 4. At terminals bb' the mutual impedances were taken to be the same as for short dipoles [5]. This approximation is justified by the slow change in pattern characteristics

Table 1 — Dipole Lengths in a 16-Element Backward Wave Yagi Array

Backward-Wave Dipoles		Yagi Director Dipoles	
Element	Length (m)	Element	Length (m)
1	0.780	6	0.340
2	0.660	7	0.380
3	0.680	8	0.340
4	0.650	9	0.340
5	0.560	10	0.340
		11	0.340
		12	0.300
		13	0.300
		14	0.300
		15	0.290
		16	0.280

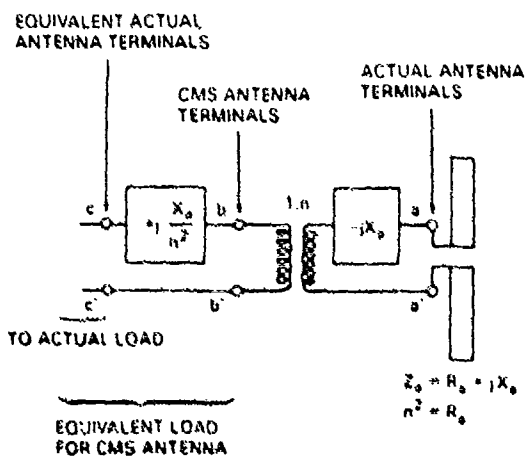


Fig. 4 — Equivalent circuit for dipole calculations

for dipole antennas less than 1 wavelength in overall length [4]. The dimensions of the dipole then enter the calculations only through their effect on the individual dipole input impedance.

H-plane antenna patterns were computed at free-space wavelengths from 0.940 to 1.060 m. Patterns in the 8% band from 0.960 to 1.040 m are shown in Figs. 5a and 5b.

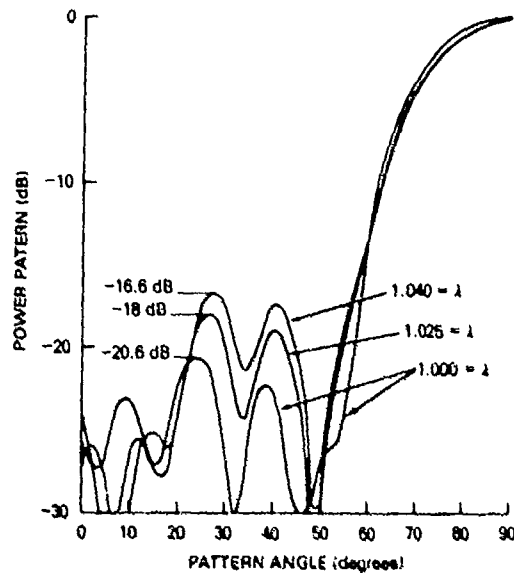


Fig. 5a — H-plane radiation patterns for the 16-element antenna of Table 1 computed at the free-space wavelengths indicated

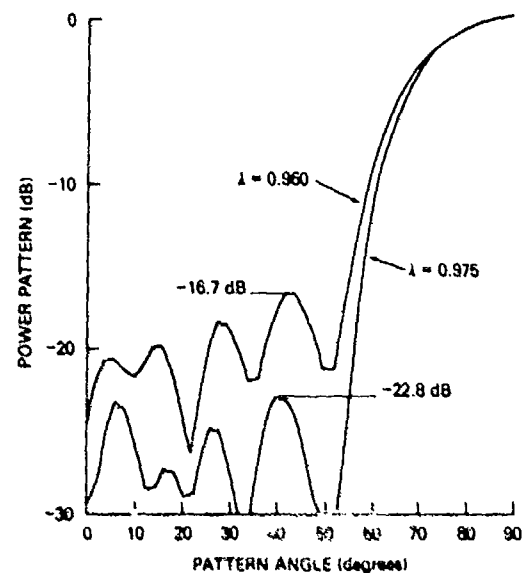


Fig. 5b — H-plane radiation patterns for the 16-element antenna of Table 1 computed at the free-space wavelengths indicated

Within this band, sidelobes remain below -16.6 dB. The sidelobe level deteriorates to -14 dB at the edges of a 10% band. The dipole element pattern assures that E-plane patterns have sidelobes at least 2.5 dB lower than the corresponding H-plane patterns. Radiation for negative angles (backward lobes) was not computed explicitly.

ACKNOWLEDGMENTS

The author is grateful to Dr. T. L. ap Rhys for his interest and valuable comments.

REFERENCES

1. W.K. Kahn, "Center-fed Leaky-Wave Yagi Hybrid Antenna," Navy Technical Disclosure Bulletin 3 (No. 8), 60-62 (Aug. 1978).
2. D.E. Isbell, "Log-Periodic Dipole Arrays," IRE Transactions on Antennas and Propagation AP-8 (No. 3), 260-267 (May 1960).
3. H.W. Ehrenspeck and H. Poehler, "A New Method for Obtaining Maximum Gain from Yagi Antennas," IRE Transactions on Antennas and Propagation AP-7 (No. 4), 379-386 (Oct. 1959).
4. H. Jasik, editor, *Antenna Engineering Handbook*, McGraw-Hill, New York, 1961, Section 16.

NRL REPORT 8377

5. W.K. Kahn and W. Wasykiwskyj, "Coupling Radiation and Scattering by Antennas," Proceedings MRI Symposium on Generalized Networks, Vol. XVI, Polytechnic Institute of Brooklyn, Apr. 1966, pp. 83-114.
6. A.C. Gately, Jr., D.J.R. Stock, and B. Ru-Shao Cheo, "A Network Description for Antenna Problems," Proceedings IEEE 56, 1181-1193 (July 1968).
7. H.A. Wheeler, "Transmission Lines and Equivalent Networks-Wheeler Monograph No. 1," Wheeler Monographs, Vol. I, Wheeler Laboratories Div. of Hazeltine Corp., New York, 1953.
8. E.C. Jordan and K.G. Balmain, "Electromagnetic Waves and Radiating Systems," 2nd edition, Prentice Hall, Englewood Cliffs, N.J., 1968.